Role of the inter-ply microstructure in the consolidation quality of high-performance thermoplastic composites

R. Arquier, H. Sabatier, Ilias Iliopoulos, G. Régnier, G Miquelard-garnier

Received: 3 June 2023 | Revised: 7 September 2023 | Accepted: 29 September 2023

DOI: 10.1002/pc.27847

RESEARCH ARTICLE

spe INSPIRING PLASTICS PROFESSIONALS Polymer COMPOSITES WILEY

Role of the inter-ply microstructure in the consolidation quality of high-performance thermoplastic composites

R. Arquier | **H. Sabatier** | **I. Iliopoulos** | **G. Régnier** | **G. Miquelard-Garnier**

Laboratoire PIMM, Arts et Métiers Institute of Technology, CNRS, Cnam, HESAM Universite, Paris, France

Correspondence
G. Miquelard-Garnier, Laboratoire PIMM, Arts et Métiers Institute of Technology, CNRS, Cnam, HESAM Universite, 151 Boulevard de l'Hôpital, Paris 75013, France.
Email: guillaume.miquelardgarnier@lecnam.net

Funding information
Bpifrance, Grant/Award Number: PSPC. AAP-7.0_HAICoPAS

Abstract

Consolidation of Carbon Fiber (CF)/high-performance thermoplastic composites is much less understood than the one of their thermoset counterparts. It is usually assumed that the consolidation quality is directly linked to the removal of voids within the sample during consolidation, leading to mechanical properties suitable for aerospace applications. A systematic study of the temporal evolution of CF/polyetherketoneketone (PEKK) samples' microstructure consolidated under low pressure in a rheometer is related to the increase in interlaminar shear strength. The results show that despite similar void contents well-below 1 vol%, samples can present significant differences in ILSS values, from 80 to 95 MPa for cross-ply samples, and from 98 to 112 MPa for unidirectional (UD) ones. A microstructural analysis shows that, for these materials, consolidation quality is rather related to a reorganization of the inter-ply, a resin-rich (∼70 vol%) region of typical thickness 10 μm which is slowly repopulated in fibers during consolidation.

Highlights

- Microstructure of CF/PEKK composites is characterized over consolidation time
- Contrary to thermosets void content cannot be used to predict mechanical properties
- ILSS increase over consolidation time is related to inter-ply reorganization
- Inter-ply microstructure and ILSS have a direct correlation
- The repopulation in fibers of the resin-rich inter-ply is a slow process

KEYWORDS
carbon fiber, consolidation, interface/interphase, interfacial strength, thermoplastic resin

1 | INTRODUCTION

High-performance thermoplastic composites, that is, thermoplastics reinforced by a high volume fraction (∼ 60 vol%) of continuous CF, gain interest over more well-known thermoset-based ones especially for aerospace applications because of their possibility to be welded or recycled.[1–3] Among other thermoplastics commonly used in the aerospace industry, glassy polyetherimide (PEI), and polyethersulfide (PES) or semi-crystalline polyphenilsulfide

(PES),[4] polyaryletherketones (PAEK) are natural candidates for structural applications due to the wide temperature range at which they can be used, their (relative) ease of processability, high chemical, thermomechanical and oxidative resistance as well as good impact properties.[3,5,6] Polyetheretherketone (PEEK), whose structure consists in the repetition of two ether groups and one ketone has been the most studied and used PAEK so far.[3,7] The presence of ether groups leads to lower melting temperature (hence make them easier to process than other polymers of the same family, such as polyetherketone (PEK)).

Processing these materials consist, both in the case of thermosets and thermoplastics, in stacking prepreg,[8] single plies (called tapes) with typical thicknesses of 200 μm,[3] generally using Automated Tape Placement (ATP). The assembly is then being consolidated in an autoclave or under a press, with applied pressures of 7–10 bar.[9,10] For economic reasons, in-situ consolidation through ATP or the use of out-of-autoclave (OOA) devices, such as vacuum bag only (VBO) with lower pressures applied (∼ 1 bar)[11] are now considered for this last step.[12–14] The goal of this consolidation step is to facilitate flow in the composite, which lowers the void content of the composite and in turn increases its mechanical properties.

Thermoset-based composites consolidation in autoclaves is now well-understood theoretically[15,16] and well-mastered in the industry,[17] as the void removal is favored by the low viscosities[2] and high pressures applied. For these materials, the increase in mechanical properties in the course of consolidation is generally directly linked to a decrease in the void content.[18–20] To achieve the targeted mechanical properties, sufficient adhesion between plies in the composite is needed, and can be characterized by different methods such as double cantilever beam (DCB),[21] peel tests,[22] lap shear strength (LSS)[23] or interlaminar shear strength (ILSS). A linear relationship between ILSS and void content has for example been evidenced long ago[24] for CF/epoxy composites. Hence, a validation of the consolidation quality is often obtained directly through the measurement of the void content for these thermoset-based composites.

When the pressure is lowered, such as in VBO processes, consolidation is much more difficult.[25,26] This is even more the case for high-performance thermoplastics, which require much higher processing temperatures and display viscosities 10 to 100 times higher than thermosets.[2] Recent studies have focused on the void removal in high-performance thermoplastic composites[27,28] whether in autoclave or out-of-autoclave processes, and have proposed directions for optimizing the process or the tape architecture.[29]

However, it is unclear if void removal in thermoplastic composites is as directly related to the improvement of mechanical properties as in thermoset ones. Though approaches have been developed to measure for example the fracture behavior of continuous fibers reinforced composite laminates,[30,31] no systematic study has been conducted yet on these materials to link the improvement of the mechanical properties with the microstructural evolution during consolidation.

Hence, we propose an approach where consolidation is conducted on carbon CF/PEKK samples under a rheometer, which allows to reproduce consolidation cycles similar to VBO, as well as to easily perform interrupted tests (i.e., vary the consolidation time). PEKK has been chosen because it has gained interest recently over PEEK as a matrix for composites that can have potential use in the production of future aerospace primary structures.[7,32,33] Its melting temperature can be lowered without reducing its service temperature,[34] along with a better control of its crystallinity,[35,36] by tuning the ratio between terephtaloyl (para) and isophtaloyl (meta) isomers (T/I ratio). Systematic characterizations of the microstructure are then conducted as a function of consolidation time, not only in terms of voids content but also of inter-ply morphology. These microstructural evolutions are finally linked to the variations of ILSS as a function of the consolidation time, and discussed in terms of consolidation quality.

2 | EXPERIMENTAL

2.1 | Materials

The UD 200 μm – thick tapes used in this study have been kindly provided by Hexcel. The matrix used is a PEKK from Arkema with a 70/30 T/I ratio and a molecular weight close to 70 kg/mol. It has a glass transition temperature $T_g = 162°C$, a melting temperature $T_m = 332°C$ and a Young's modulus $E \approx 3.8$ GPa.[37] The fibers are unsized[38] continuous Hexcel High strength 7 μm – diameter carbon fibers AS7 ($E \approx 240$ GPa, tensile strength ≈ 5 GPa[39]). The tapes have an initial void content and fiber volume fraction close to 5 and 60 vol% respectively (as given by the supplier, and verified using the ImageJ (NIH) software).

2.2 | Consolidation model experiment

A total of 16 tapes are first cut in 25 mm – diameter disks and then assembled manually to form either UD $[0]_{16}$ or cross-ply $[0/90]_{4s}$ stackings. A 50 μm – thick polyimide (PI) film is placed between the composite and the 25 mm stainless steel rheometer plates to prevent the samples from sticking to the plates. An Anton Paar MCR 502 rheometer equipped with 25 mm diameter circular plates is used to apply a consolidation temperature–

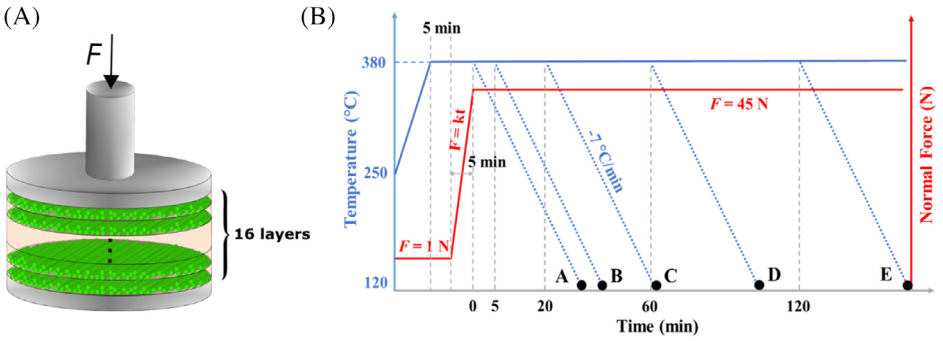

FIGURE 1 (A) Schematic of the consolidation experiment with the rheometer for the UD configuration. (B) Temperature–pressure–time consolidation cycles of the study.

pressure–time cycle similar to those found in VBO processes (Figure 1A).[28,40]

A typical cycle is described in Figure 1B. A ramp of temperature between 250 and 380°C at 15°C/min is conducted under a 1 N force to maintain contact between plies. Next, the sample is let 5 min at 380°C under 1 N force to ensure the temperature is homogeneous throughout the sample. Then a ramp of force is applied during 5 min until 45 N is reached, corresponding to a pressure of 0.92 bar, similar to the one encountered in VBO.[11] For both UD and cross-ply stackings, the consolidation is stopped at various times, that is, 0, 5, 20, 60 or 120 min (corresponding to A, B, C, D, and E respectively in Figure 1B) before being cooled down at −7°C/min, similar to VBO cooling rates. All the experiments are conducted under nitrogen flow (N_2) to avoid possible degradation due to oxygen (similar to vacuum in VBO).

The stability of the matrix during the consolidation has been verified by thermogravimetric analysis (TGA). No significant thermal degradation has been evidenced after 3 h at 380°C under N_2 (Figure S1) with less than 1% mass loss mostly occurring during the first 30 min (mainly due to the evaporation of water absorbed by the matrix). It has also been verified by DSC that the cooling cycle used in this study is slow enough to allow full crystallization of the matrix (Figure S2), hence it will be assumed crystallinity plays no role in the different results discussed in the following.

2.3 | VBO consolidation

Vacuum bag only consolidation was conducted using a lab-made set-up. Briefly, the 150 × 150 mm cross-ply samples are prepared by stacking manually 24 tapes ($[0/90]_{6s}$) and placed on a flat stainless-steel surface between anti-adhesive release films. A breather is placed on top of the sample to ensure homogeneous gas diffusion. The whole system is covered by a vacuum bag and then installed in an oven able to control the temperature and pressure in the bag. Once a vacuum below 50 mbar is achieved, a ramp between room temperature and the final set temperature (varied between 375 and 390°C) is performed at 7°C/min. The temperature remains then constant for a given time (varied between 50 min and 2 h) before a cooling ramp at 7°C/min. For each condition, 3 samples were tested. The temperature of the samples can be monitored with thermocouples placed at different locations (Figure S3).

2.4 | Mechanical characterization

To assess the consolidation quality, Interlaminar Shear Strength (ILSS) is determined with the short-beam shear test (SBS). ILSS is a measurement of the composite resistance under shear parallel to the plies, and can be viewed as a characterization of the "quality" of the interfaces. Note that what is obtained with SBS is actually the short-beam strength, which is an analogue for ILSS but not an exact measure, due to the complex state of stress instead of pure shear. From the consolidated samples obtained with the previously described experiments, two bars with dimensions following ASTM D2344[41] are cut using a diamond wire saw from Escil, allowing to run two ILSS measurements for each stacking and consolidation time. SBS is performed using an INSTRON 5581, with a cell force of 50 kN. A compression rate of 1 mm/min is applied on the sample and the maximum force before rupture F_R is extracted to obtain ILSS value through Equation 1:

$$ILSS = \frac{3F_R}{4le} \quad (1)$$

where l and e are the width and thickness of the bars respectively (see Figure S4a).

Figure S4b shows typical stress-displacement curves for the cross-ply $[0/90]_{4s}$ composites consolidated at different times where a sharp rupture with low plasticization can be observed for all samples, consistent with ASTM recommendations.[41]

2.5 | Microstructural characterization

From the consolidated samples, two small samples (1 mm width) for each stacking are also cut by a diamond wire saw from Escil for microscopic observations. For both the cross-ply and UD composites, the cut is made at 45° toward the fiber direction in order to ease the samples' preparation and observation. These samples are then mounted using an Epofix resin from Struers with a cure time of 12 h at room temperature and polished on Mecatech 334 from Presi using a polishing cycle consisting of a first step with silicon carbide foils from Struers with grain sizes from 400 to 2400, followed by the use of diamond solutions with lubricants (with particle sizes in suspension from 9 to 0.25 μm).

Void content is characterized by analyzing optical microscopy images obtained with an Axio microscope (Zeiss) equipped with a ×10 objective (×100 magnification). The 8-bit 1388×1088 pixels images are treated with ImageJ. An optimization of the brightness and contrast is first realized and an automatic Image J threshold pixel value is selected to enable the binarization of the image, with {fibers + matrix} in white (pixel value equals to 1) and the voids in black (pixel value equals to 0). The void content (for voids that have typical dimensions bigger than the pixel size, i.e., > 1 μm) is defined as the ratio between the selected particles and the total area of the analyzed image. The obtained values are averaged on 8 images (4 images × 2 samples) per stacking and consolidation time. The images are taken randomly throughout the sample. The error bars in the following will correspond to the confidence interval at 95% toward the average, obtained with 8 experimental values.

In the following, the inter-ply microstructure will also be characterized since it is well known that a matrix interlayer is naturally present at the inter-ply for cross-ply stackings.[42] Specifically, the thickness of the inter-ply as well as its mean fiber content will be evaluated. To do so, we developed a different protocol than the one previously described: this time, an automatic Image J threshold is conducted to separate the fibers from {matrix + voids}, before binarization of the image, leading to white fibers and black {matrix + voids}. Then the ratio between white pixels and the total number of pixels is calculated for each horizontal pixel (0.9 μm) line. In other words a mean fiber volume fraction defined as ([fiber content/(fiber content + resin content + void content)]×100) is calculated for each horizontal pixel line with the plies stacked vertically (see Supplementary movie 1). To smoothen the signal, the ratio for each pixel line is averaged with the one above and below this line. The analyses are performed on 6 images (containing each at least 5 inter-plies) per stacking and consolidation time, meaning an average on more than 30 inter-plies. Mean values as well as their confidence interval at 95% are then calculated.

3 | RESULTS AND DISCUSSION

From Equation 1, the ILSS values of the $[0]_{16}$ and $[0/90]_{4s}$ consolidated composites at 380°C and 0.92 bar can be compared at various consolidation times (Figure 2). It is seen that in both cases ILSS values increase with the consolidation time, with similar trends, that is, a sublinear increase over time. However, the relative increase over 2 h of consolidation is much more pronounced for the cross-ply composites (+50%) than for the UD ones (+15%). It is also seen that while UD samples will reach typical ILSS values targeted for aerospace applications similar to those obtained in autoclave consolidation (105 MPa)[9,11,43] in less than 1 h, much longer times (2 h or more) are needed for cross-ply samples (95 MPa).

3.1 | Void content characterization

Let us first consider, analogous to the case of thermoset composites, the evolution of the void content for each stacking and consolidation time in the case of CF/PEKK composites. Figure 3 shows typical images of the microstructural evolution over time for the UD and cross-ply composites at 0, 20, and 120 min. As expected, the number and size of voids, shown in red circles in Figure 3,

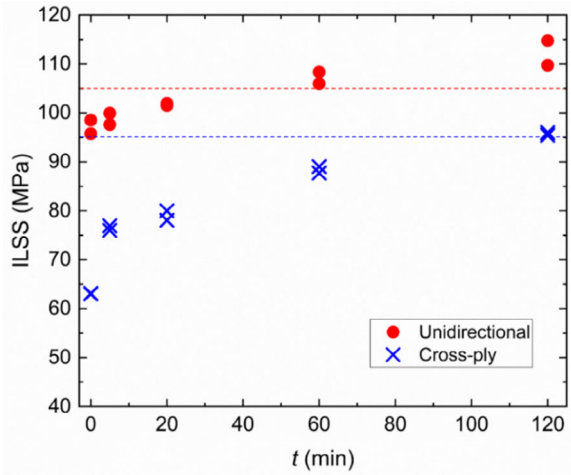

FIGURE 2 ILSS values for $[0]_{16}$ and $[0/90]_{4s}$ CF/PEKK composites at 380°C and 0.92 bar and different consolidation times (0, 5, 20, 60, and 120 min). The dashed lines represent the typical target values for cross-ply (95 MPa) and UD composites respectively (105 MPa).

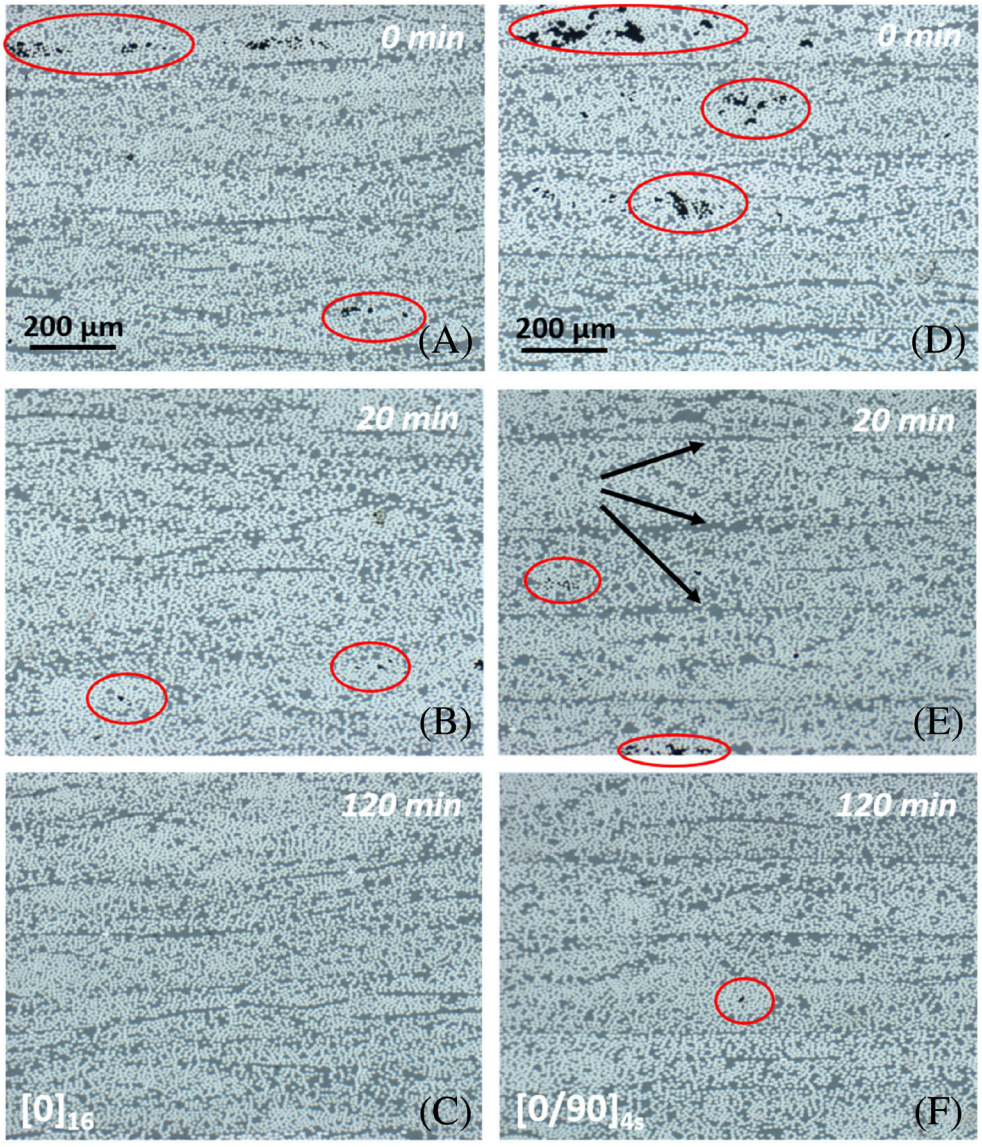

FIGURE 3 Typical optical microscopy images of the microstructure of $[0]_{16}$ (A, B, C) and $[0/90]_{4s}$ (D, E, F) CF/PEKK composites consolidated for 0, 20, and 120 min respectively. The fibers are in bright gray, the matrix in gray and the voids in black (circled in red). Scale bar is identical for all images.

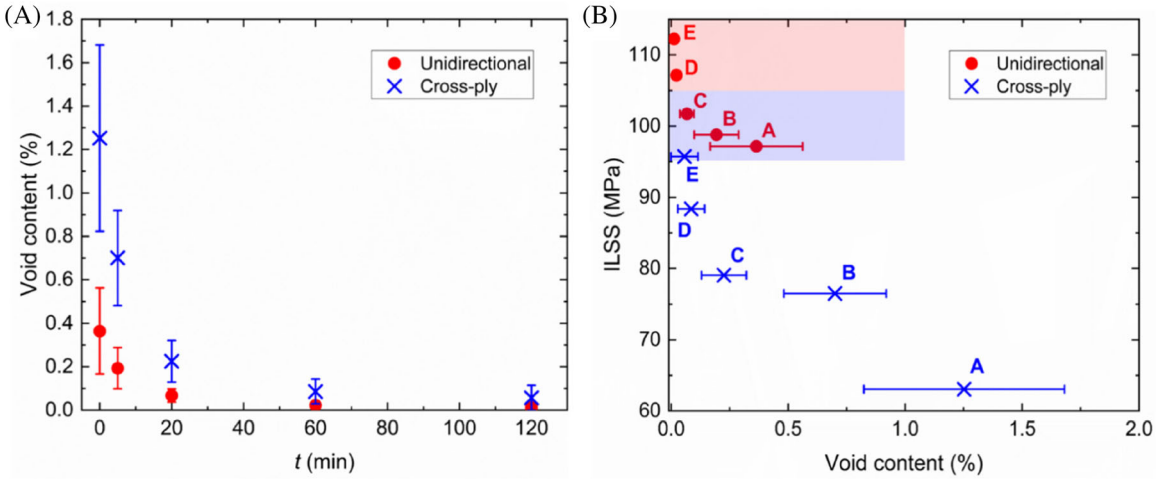

FIGURE 4 (A) void content as a function of consolidation time for UD and cross-ply composites; (B) ILSS as a function of the void content. The ILSS value presented here (and in the following figures) for a given condition is the average of the two values shown in Figure 2. The pale blue and red colors in the upper part of panel (b) highlight the regions fulfilling aerospace criteria for cross-ply and UD composites respectively (void content below 1%, ILSS higher than 95 MPa for cross-ply composites, higher than 105 MPa for UD ones). A, B, C, D, and E are samples with different consolidation times as shown in Figure 1 (0, 5, 20, 60 and 120 min respectively).

decreases with the consolidation time. Also, these voids, even at the beginning of the consolidation (Figure 3A,D), are almost only located within the plies and not at the ply-ply interface (black arrows in Figure 3E).

Using these images, a quantitative analysis allows to follow the void content evolution with the consolidation time (Figure 4A). The corresponding ILSS as a function of the void content is then presented in Figure 4B for UD (in red) and cross-ply (in blue) composites. The void content decreases rapidly (in a few minutes) to values far below 1 vol% for both types of composites, a value usually set as a criterion of consolidation quality in the aerospace industry for thermosets composites.[44] The few remaining voids are located in between closely packed fibers at the intra-plies.

Yet, important variations of the ILSS values can still be observed for void contents well-below this 1% threshold (see Figure 4B). For example, while the samples show a difference of only 0.1% in void content (from 0.2% to 0.1%), the ILSS values can display differences of 13% for UD composites and more than 20% for cross-ply ones. Moreover, even for very low void contents (below 0.2%), only a few composites (the ones at longer consolidation times) reach sufficient ILSS values (about 105 MPa for UD and 95 MPa for cross-ply, as stated earlier).

Hence, contrary to thermosets, the void content does not seem to be a sufficient criterion to characterize the consolidation quality of a thermoplastic composite. To go further, the evolution of the microstructure at the ply-ply interface will be discussed in the following.

3.2 | Inter-ply characterization

The image analysis proposed in the Materials and Methods section (see Section 2.4 as well as Supplementary Movie 1) is used to characterize the inter-ply evolution as a function of consolidation time for both UD and cross-ply composites. From these analyses, the mean fiber volume fraction within the inter-ply as well as its thickness can be obtained. A typical analysis is presented in Figure 5. First, it should be noticed that the mean fiber volume fraction obtained within the images using this approach is in all cases ≈ 58 vol%, consistent with the supplier's information, which confirms a posteriori the validity of the proposed approach. It can also be noted that the fiber volume fraction is relatively scattered along the sample's thickness. This can be explained by the fact that the pixel size ($\lesssim 1\,\mu m$) is much smaller than the fiber size ($\approx 7\,\mu m$) (see Supplementary Movie 1). Hence, due to local heterogeneities in the dispersion/distribution of fibers within the sample, the mean fiber volume fraction along each pixel line can vary quite substantially. In the following, to distinguish inter-plies from these local variations, we will subtract to the mean fiber volume

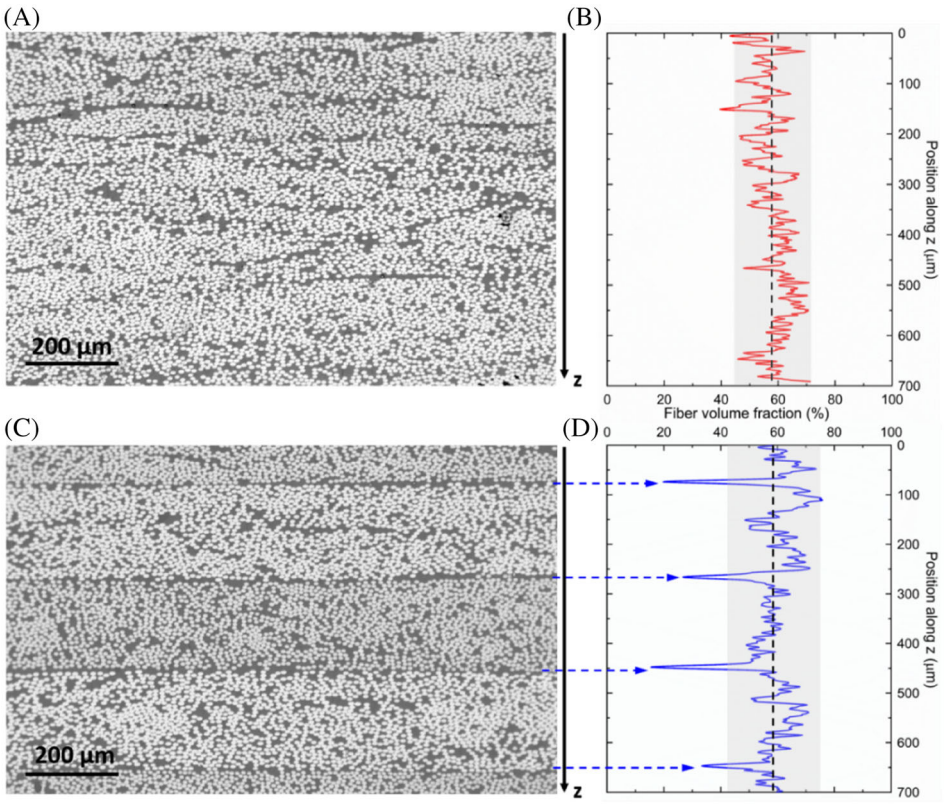

FIGURE 5 Typical microstructures of the (A) UD $[0]_{16}$ and (C) cross-ply $[0/90]_{4s}$ CF/PEKK composites after 20 min of consolidation, with the corresponding evolution of the fiber volume fraction along the depth (B and D).

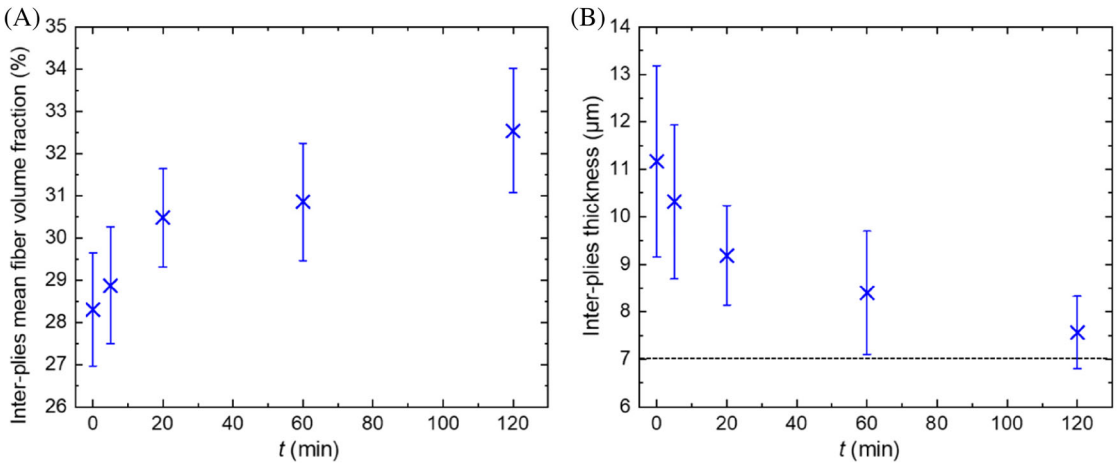

FIGURE 6 (A) Evolution of the mean fiber volume fraction and (B) the thickness of the inter-plies over consolidation time for $[0/90]_{4s}$ CF/PEKK composites. The dotted line in panel (b) is set at the fiber diameter.

fraction the difference between the maximum and the mean. The inter-plies are then defined by the peaks below this region (gray area in Figure 5B,D), as shown in Figure 5D.

It can be seen in Figure 5A,B. that even at short consolidation times (20 min), inter-plies can hardly be distinguished in $[0]_{16}$ laminates. This confirms the possibility of fibers redistribution from one ply to another for these UD stackings at relatively short times, due to a global {matrix + fiber} flow transverse to the fibers as pressure is applied.[45] This can then be linked to the high ILSS values obtained even for the short consolidation times, with target values reached shortly after 20 min.

Let us now focus on the inter-plies in the $[0/90]_{4s}$ composites. As can already be seen in both Figure 3E and 5C, the inter-plies are still visible in these systems after 20 min, and well-defined peaks can be obtained using the proposed analysis (Figure 5D). The width of the peaks, which is in other words the thickness of the inter-plies, can then be extracted from the image, as well as the mean fiber volume fraction in the inter-plies. It is then possible to follow the evolution of both of these quantities (Figure 6A,B respectively) over consolidation time.

There is an increase of the mean fiber volume fraction of about 15% as the consolidation time varies from 0 to 120 min. The inter-ply enriches in fibers over consolidation time, that is, as pressure is applied at high temperature, suggesting that though more localized than for UD composites, a reorganization at the ply-ply interface occurs. Still, it can be noted that after 2 h of consolidation, the mean fiber volume fraction in the inter-ply is only slightly higher than 30 vol%, much lower than the mean fiber volume fraction in the whole composite (58 vol%). In parallel, Figure 6B shows a clear decrease of the inter-plies thickness with consolidation time. After 120 min, the typical size of the inter-plies is close to the fiber diameter (7 µm). Both observations are consistent with fiber locking,[46,47] occurring when fibers of different orientations are in close contact, and preventing from further interfacial reorganization.

Finally, we can look at the ILSS variation as a function of the ply-ply interface evolution for the cross-ply composites (Figure 7). Figure 7A shows the evolution of ILSS as a function of the mean fiber volume fraction in the inter-plies. A linear trend is observed, with a target value (95 MPa) reached for a fiber volume fraction of about 32 vol%. A linear trend is also observed concerning the increase of ILSS as the inter-plies thickness decrease (Figure 7B), the target value (95 MPa) being reached for thicknesses close to 8 µm.

As the time spent by the composite at high temperature and pressure increases, the fibers progressively rearrange themselves within the matrix layer at the inter-plies. They can therefore contribute more and more to the resistance of the composite to the interlaminar shear generated during the ILSS tests.

One should note that if the evolution of ILSS with either the fiber volume fraction in the inter-plies or their thickness is linear ($R^2 \approx 0.89$ and 0.95 respectively) and rather sharp (a 50% increase in ILSS for a fiber volume fraction at the inter-plies increasing only from 27 to 32%v), this is not the case with time, as the evolution of these properties with time is observed to follow a logarithmic trend in the time range studied (see Figure S5). Hence, the reorganization of the inter-plies is a slow process, and a good consolidation quality can only be achieved after long times for these highly viscous thermoplastic composites.[45,48] A detailed modeling of the local flows at the inter-plies that could account for these trends shall be the aim of future work but it can be understood qualitatively that as the resin-rich inter-ply region becomes more

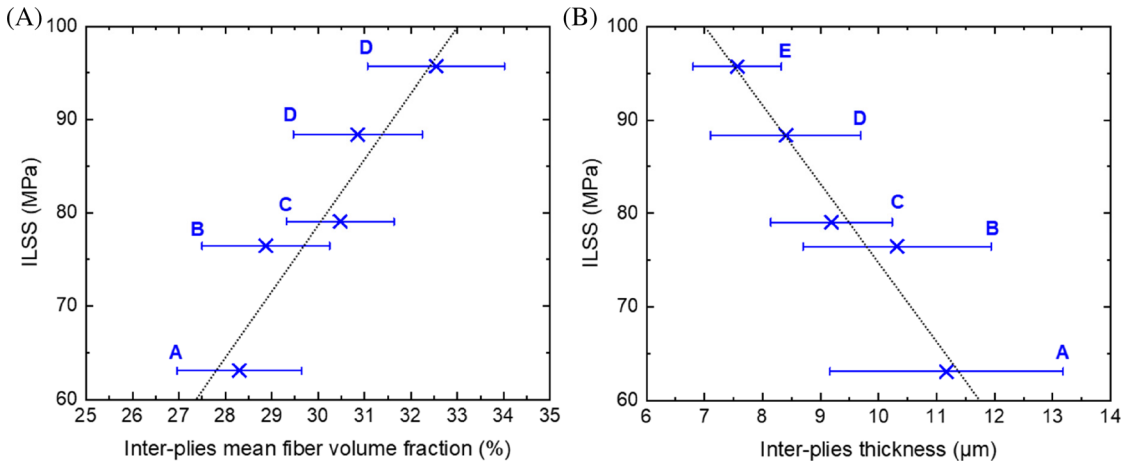

FIGURE 7 ILSS evolution as a function of (A) the mean fiber volume fraction at the inter-plies and (B) the inter-plies thickness for the $[0/90]_{4s}$ consolidated composites. Dashed lines are linear fits. A, B, C, D, and E are for samples with different consolidation times as shown in Figure 1 (0, 5, 20, 60, and 120 min respectively).

populated with fibers, the viscosity of this interfacial layer will increase, while its thickness will decrease, resulting in a local flow that will become slower over time. The resulting changes in properties shall then, vary sub-linearly with time, which is consistent with our experimental observations.

Finally, one can wonder if the behavior observed with the consolidation under the rheometer effectively describes what happens during VBO consolidation. To answer this question, a set of complementary VBO consolidation experiments was performed on 150 × 150 mm [0/90]6 s (24 plies) plates. It is seen in Figure S6a that VBO consolidations indeed take much longer times (in terms of consolidation quality) than rheometer ones, due to the thermal inertia of the VBO process (see Figure S3b). Despite this shift in consolidation time, it is also clear that the evolution of ILSS as a function of time follows the same logarithmic trend (Figure S6b), indicating similar mechanisms at play in both consolidations.

4 | CONCLUSION

Consolidation has been conducted on UD $[0]_{16}$ or $[0/90]_{4s}$ CF/PEKK composites under a rheometer, with a pressure of 0.92 bar and a temperature of 380°C, close to the VBO parameters for these materials. Varying consolidation times up to 2 h have been applied, and ILSS measurements have been linked to the composites' microstructure characterized by image analysis, both in terms of void content and inter-ply morphology (thickness and fiber content).

This study demonstrates that, contrary to thermosets composites, the void content evolution during consolidation cannot be directly related to the ILSS values for high-performance thermoplastic composites such as CF/PEKK. Low void contents are rapidly reached (10–20 min) during consolidation at 1 bar even for these very viscous materials. Although a sufficiently low porosity level is necessary to provide good mechanical properties (criterion fixed at 1% by the aerospace industry based on thermosets materials), it is seen that important ILSS variations can still be observed for thermoplastic composites with void contents well-below this criterion. Remaining voids are indeed located within the plies whereas the ILSS is a measurement of the quality of the ply-ply interface.

The evolution of the {fiber + matrix} repartition at the inter-plies appears to be the governing parameter to assess the consolidation quality of high-performance thermoplastic composites. Concerning UD configuration, global reorganization of the composite during consolidation leads rapidly to a homogeneous {fiber + matrix} repartition through the whole sample's thickness, resulting in ILSS target values reached after about 30 min of consolidation. On the contrary, the resin-rich inter-plies for cross-ply composites remain clearly visible even after 2 h of consolidation. While the mean fiber volume fraction at the inter-plies increase and the thickness of the inter-plies decreases with the consolidation time, this reorganization, related to the increase in the ILSS, is slow.

Optimizing consolidation of high-performance thermoplastic composites would then mean designing tapes with such architecture that this local reorganization of the inter-plies is facilitated and quicker,[49] to reduce the

consolidation time, which is an important objective especially for VBO process.

ACKNOWLEDGMENTS

This work was conducted under the framework of HAICoPAS, a PSPC project (projet de recherche et développement structurant pour la compétitivité) and of the Industrial Chair Arkema (Arkema/ CNRS-ENSAM-Cnam). BPI France is acknowledged for funding the PhD work of R. Arquier (project number: PSPC. AAP-7.0_HAICoPAS). The authors would like to thank Arkema, Hexcel, and more specifically Lucien Fiore, Nicolas Cadorin, Michel Glotin, Jean-Paul Moulin, Henri-Alexandre Cayzac, Jérôme Pascal and Yves Deyrail for fruitful discussions. We finally thank Anna Dmochowska for her help in designing the schematic proposed in Figure 1.

DATA AVAILABILITY STATEMENT

The data that support the findings of this study are available from the corresponding author upon reasonable request.

ORCID

I. Iliopoulos https://orcid.org/0000-0002-9368-2906
G. Régnier https://orcid.org/0000-0002-1543-1837
G. Miquelard-Garnier https://orcid.org/0000-0002-0251-8941

REFERENCES

1. Clyne TW, Hull D. *An Introduction to Composite Materials*. 2nd ed. Cambridge Solid State Science Series; 2019.
2. Vaidya UK, Chawla KK. Processing of fibre reinforced thermoplastic composites. *Int Mater Rev*. 2008;53:185-218. doi:10.1179/174328008X325223
3. Arquier R, Iliopoulos I, Régnier G, Miquelard-Garnier G. Consolidation of continuous-carbon-fiber-reinforced PAEK composites: a review. *Mater Today Commun*. 2022;32:104036. doi:10.1016/j.mtcomm.2022.104036
4. Barile M, Lecce L, Iannone M, Pappadà S, Roberti P. *Thermoplastic Composites for Aerospace Applications. Revolutionizing Aircraft Materials and Processes*. Springer; 2020:87-114. doi:10.1007/978-3-030-35346-9_4
5. Choupin T, Fayolle B, Régnier G, Paris C, Cinquin J. A more reliable DSC-based methodology to study crystallization kinetics: application to poly (ether ketone ketone) (PEKK) copolymers. *Polymer*. 2019;155:109-115. doi:10.1016/j.polymer.2018.08.060
6. Sukur EF. Thermally conditioned aerospace-grade carbon fiber reinforced polyether ketone ketone composites: structure, impact response, and thermomechanical performance. *Polym Compos*. 2023;44:2530-2544. doi:10.1002/pc.27261
7. Li S, Zhang Y, Chen W, Chen L, Fang G, Peng F. Dynamical mechanical analysis of continuous carbon fiber-reinforced polyetheretherketones under multi-consecutive temperature scans. *Polym Compos*. 2022;43:6013-6024. doi:10.1002/pc.26900
8. Li B, Zhang F, Jiao M, Li Y, Wang X, Zhang X. Carbon fiber/polyetherketoneketone composites. Part I: an ideal and uniform composition via solution-based processing. *Polym Compos*. 2022;43:2803-2811. doi:10.1002/pc.26577
9. Lystrup A, Andersen TL. Autoclave consolidation of fibre composites with a high temperature thermoplastic matrix. *J Mater Process Technol*. 1998;300:80-85. doi:10.1016/s0924-0136(97)00398-1
10. Manson JE, Schneider TL, Seferis JC. Press-forming of continuous-fiber-reinforced thermoplastic composites. *Polym Compos*. 1990;11:11-120. doi:10.1002/pc.750110207
11. Saffar F, Sonnenfeld C, Beauchêne P, Park CH. In-situ monitoring of the out-of-autoclave consolidation of carbon / poly-ether-ketone-ketone prepreg laminate. *Front Mater*. 2020;7:1-12. doi:10.3389/fmats.2020.00195
12. Martin I, Saenz Del Castillo D, Fernandez A, Güemes A. Advanced thermoplastic composite manufacturing by in-situ consolidation: a review. *J Compos Sci*. 2020;4:1-36. doi:10.3390/jcs4040149
13. Donough MJ, Shafaq S, John NA, Philips AW, Gangadhara Prusty B. Process modelling of in-situ consolidated thermoplastic composite by automated fibre placement – a review. *Compos Part A Appl Sci Manuf*. 2022;163:107179. doi:10.1016/j.compositesa.2022.107179
14. Heathman N, Koirala P, Yap T, Emami A, Tehrani M. In situ consolidation of carbon fiber PAEK via laser-assisted automated fiber placement. *Compos B Eng*. 2022;249:110405. doi:10.1016/j.compositesb.2022.110405
15. Barari B, Simacek P, Yarlagadda S, Crane RM, Advani SG. Prediction of process-induced void formation in anisotropic fiber-reinforced autoclave composite parts. *Int J Mater Form*. 2020;13:143-158. doi:10.1007/s12289-019-01477-4
16. Li M, Tucker CL. Modeling and simulation of two-dimensional consolidation for thermoset matrix composites. *Compos Part A Appl Sci Manuf*. 2002;33:877-892. doi:10.1016/S1359-835X(02)00017-9
17. Min L, Charles LT. Optimal curing for thermoset matrix composites: thermochemical and consolidation considerations. *Polym Compos*. 2002;23:739-757.
18. Guo ZS, Liu L, Zhang BM, Du S. Critical void content for thermoset composite laminates. *J Compos Mater*. 2009;43:1775-1790. doi:10.1177/0021998306065289
19. Leali Costa M, De Almeida S, Cerqueira RM. The influence of porosity on the interlaminar shear strength of carbon/epoxy and carbon/bismaleimide fabric laminates. *Compos Sci Technol*. 2001;61:2101-2108.
20. Di Landro L, Montalto A, Bettini P, Guerra S, Montagnoli F, Rigamonti M. Detection of voids in carbon/epoxy laminates and their influence on mechanical properties. *Polym Polym Compos*. 2017;25:371-380. doi:10.1177/096739111702500506
21. Avenet J, Levy A, Bailleul J, Le Corre S, Delmas J. Adhesion of high performance thermoplastic composites: development of a bench and procedure for kinetics identification. *Compos Part A Appl Sci Manuf*. 2020;138:106054. doi:10.1016/j.compositesa.2020.106054
22. Khan MA, Mitschang P, Schledjewski R. Identification of some optimal parameters to achieve higher laminate quality through tape placement process. *Adv Polym Technol*. 2010;29:98-111. doi:10.1002/adv.20177
23. Stokes-Griffin CM, Compston P. Investigation of sub-melt temperature bonding of carbon-fibre/PEEK in an automated laser tape placement process. *Compos Part A Appl Sci Manuf*. 2016;84:17-25. doi:10.1016/j.compositesa.2015.12.019

24. Yoshida H, Ogasa T, Hayashi R. Statistical approach to the relationship between ILSS and void content of CFRP. *Compos Sci Technol*. 1986;25:3-18. doi:10.1016/0266-3538(86)90018-7
25. Stadler H, Kiss P, Stadlbauer W, Plank B, Burgstaller C. Influence of consolidating process on the properties of composites from thermosetting carbon fiber reinforced tapes. *Polym Compos*. 2022;43:4268-4279. doi:10.1002/pc.26687
26. Lukaszewicz DHJA, Potter KD, Eales J. A concept for the in situ consolidation of thermoset matrix prepreg during automated lay-up. *Compos B Eng*. 2013;45:538-543. doi:10.1016/j.compositesb.2012.09.008
27. Patou J, Bonnaire R, De LE, Bernhart G. Influence of consolidation process on voids and mechanical properties of powdered and commingled carbon/PPS laminates. *Compos Part A Appl Sci Manuf*. 2019;117:260-275. doi:10.1016/j.compositesa.2018.11.012
28. Swamy JN, Grouve WJB, Akkerman R. An experimental study on the role of different void removal mechanisms in VBO processing of advanced thermoplastic composites. *J Reinf Plast Compos*. 2023;1-12. doi:10.1177/07316844231159134
29. Swamy JN, Grouve WJB, Wijskamp S, Akkerman R. Vacuum-bag-only consolidation of C/PEKK fiber placed preforms with engineered gas evacuation channels. *J Thermoplast Compos Mater*. 2023;1-18. doi:10.1177/08927057231177571
30. Tan W, Falzon BG. Modelling the nonlinear behaviour and fracture process of AS4/PEKK thermoplastic composite under shear loading. *Compos Sci Technol*. 2016;126:60-77. doi:10.1016/j.compscitech.2016.02.008
31. Schmitt-Thomas KG, Yang ZG, Malke R. Failure behavior and performance analysis of hybrid-fiber reinforced PAEK composites at high temperature. *Compos Sci Technol*. 1998;58:1509-1518. doi:10.1016/S0266-3538(97)00179-6
32. Choupin T, Fayolle B, Régnier G, Paris C, Cinquin J, Brulé B. Isothermal crystallization kinetic modeling of poly(etherketoneketone) (PEKK) copolymer. *Polymer*. 2017;111:73-82. doi:10.1016/j.polymer.2017.01.033
33. Lesimple G, Iliopoulos I, Marijon J, Fayolle B. Full characterization of water transport properties in Polyetherketoneketone (PEKK). *ACS Appl Polym Mater*. 2022;5:302-310. doi:10.1021/acsapm.2c01515
34. Veazey D, Hsu T, Gomez ED. Next generation high-performance carbon fiber thermoplastic composites based on polyaryletherketones. *J Appl Polym Sci*. 2017;134:19-21. doi:10.1002/app.44441
35. Pérez-Martín H, Mackenzie P, Baidak A, ÓBrádaigh CM, Ray D. Crystallinity studies of PEKK and carbon fibre/PEKK composites: a review. *Compos B Eng*. 2021;223:109127. doi:10.1016/j.compositesb.2021.109127
36. Pérez-Martín H, Mackenzie P, Baidak A, Brádaigh Ó, CM, Ray D. Crystallisation behaviour and morphological studies of PEKK and carbon fibre/PEKK composites. *Compos Part A Appl Sci Manuf*. 2022;159:106992. doi:10.1016/j.compositesa.2022.106992
37. Arkema. *Kepstan® PEKK 7002*. Tech Data Sheet; 2018.
38. Kantharaju S, Vinodhini J, Bhowmik S. An investigation to enhance the mechanical property of high-performance thermoplastic composite through different plasma treatment. *Polym Compos*. 2022;44:178-189. doi:10.1002/pc.27037
39. Hexcel Corporations. *HexTow® AS7 Carbon Fiber*. Tech Data Sheet; 2020.
40. Hoang V, Kwon B, Sung J, et al. Postprocessing mechanical properties of carbon fiber-reinforced thermoplastic composites. *J Thermoplast Compos Mater*. 2020;36:1-16. doi:10.1177/0892705720945376
41. Standard D 2344. *Standard Test Method for Short-Beam Strength of Polymer Matrix Composite Materials and their Laminates*. West Consohocken PA 19428-2959; 2000.
42. Cogswell FN. The processing science of thermoplastic structural composites. *Int Polym Process*. 1987;1:157-165. doi:10.3139/217.870157
43. Chanteli A, Kumar A, Peeters D, Higgins RMO, Weaver PM. Influence of repass treatment on carbon fibre-reinforced PEEK composites manufactured using laser-assisted automatic tape placement. *Compos Struct*. 2021;248:112539. doi:10.1016/j.compstruct.2020.112539
44. Van Hoa S, Duc Hoang M, Simpson J. Manufacturing procedure to make flat thermoplastic composite laminates by automated fibre placement and their mechanical properties. *J Thermoplast Compos Mater*. 2017;30:1693-1712. doi:10.1177/0892705716662516
45. Arquier R, Miquelard-Garnier G, Iliopoulos I, Régnier G. Assessing the shear viscous behavior of continuous carbon fiber reinforced PEKK composites with squeeze flow measurements. *Polym Test*. 2023;123:1-9. doi:10.1016/j.polymertesting.2023.108060
46. Barnes JA, Cogswell FN. Transverse flow processes in continuous fibre-reinforced thermoplastic composites. *Composites*. 1989;20:38-42. doi:10.1016/0010-4361(89)90680-0
47. McGuinness GB, ÓBrádaigh CM. Characterisation of thermoplastic composite melts in rhombus-shear: the picture-frame experiment. *Compos Part A Appl Sci Manuf*. 1998;29:115-132. doi:10.1016/S1359-835X(97)00061-4
48. Kishore V, Ajinjeru C, Hassen AA, Lindahl J, Kunc V, Duty C. Rheological behavior of neat and carbon fiber-reinforced poly(ether ketone ketone) for extrusion deposition additive manufacturing. *Polym Eng Sci*. 2020;60:1066-1075. doi:10.1002/pen.25362
49. Sacchetti F, Grouve WJB, Warnet LL, Villegas IF. Effect of resin-rich bond line thickness and fibre migration on the toughness of unidirectional carbon/PEEK joints. *Compos Part A Appl Sci Manuf*. 2018;109:197-206. doi:10.1016/j.compositesa.2018.02.035

SUPPORTING INFORMATION

Additional supporting information can be found online in the Supporting Information section at the end of this article.

How to cite this article: Arquier R, Sabatier H, Iliopoulos I, Régnier G, Miquelard-Garnier G. Role of the inter-ply microstructure in the consolidation quality of high-performance thermoplastic composites. *Polym Compos*. 2023;1-10. doi:10.1002/pc.27847